



Future Circular Collider

**PUBLICATION**

# Measurements of vacuum chamber at light source: Deliverable D4.2

Perez Rodriguez, Francisco Jose () *et al.*

30 January 2019



The European Circular Energy-Frontier Collider Study (EuroCirCol) project has received funding from the European Union's Horizon 2020 research and innovation programme under grant No 654305. The information herein only reflects the views of its authors and the European Commission is not responsible for any use that may be made of the information.



The research leading to this document is part of the Future Circular Collider Study

The electronic version of this FCC Publication is available on the CERN Document Server at the following URL :

<http://cds.cern.ch/record/2655291>

Grant Agreement No: 654305

# EuroCirCol

European Circular Energy-Frontier Collider Study

Horizon 2020 Research and Innovation Framework Programme, Research and Innovation Action

## MILESTONE REPORT

# MEASUREMENTS OF VACUUM CHAMBER AT LIGHT SOURCE

---

<b>Document identifier:</b>	EuroCirCol-P2-WP4-D4.2
<b>Due date:</b>	End of Month 28 (September 2017)
<b>Report release date:</b>	30.09.2017
<b>Work package:</b>	WP4 cryogenic beam vacuum system
<b>Lead beneficiary:</b>	ALBA
<b>Document status:</b>	RELEASED (V 1.0)

---

### Abstract:

Description of the test setup and the measurement conditions including any aspects that may have an impact on the quality of the raw data and analysis. Set of raw data, associated calibration data and relevant environment operation data. Preliminary summary of the analysis, discussion of the results and conclusions.

Copyright notice:

Copyright © EuroCirCol Consortium, 2015

For more information on EuroCirCol, its partners and contributors please see [www.cern.ch/eurocircol](http://www.cern.ch/eurocircol).



The European Circular Energy-Frontier Collider Study (EuroCirCol) project has received funding from the European Union's Horizon 2020 research and innovation programme under grant No 654305. EuroCirCol began in June 2015 and will run for 4 years. The information herein only reflects the views of its authors and the European Commission is not responsible for any use that may be made of the information.

**Delivery Slip**

	<b>Name</b>	<b>Partner</b>	<b>Date</b>
<b>Authored by</b>	Francis Perez Luis Gonzalez Sara Casalbuoni Paolo Chiggiato Roberto Kersevan Miguel Gil Costa	ALBA INFN KIT CERN CERN CIEMAT	01/09/17
<b>Edited by</b>	Julie Hadre Johannes Gutleber	CERN	29/09/17
<b>Reviewed by</b>	Michael Benedikt Daniel Schulte	CERN	15/09/17
<b>Approved by</b>	EuroCirCol Coordination Committee		25/09/17

**TABLE OF CONTENTS**

**1. DESCRIPTION OF THE TEST SETUP ..... 4**

1.1. ANKA LIGHT SOURCE ..... 4

1.2. BESTEX..... 6

1.2.1 FRONT END SETUP ..... 6

1.2.2 MEASUREMENT SETUP ..... 8

1.3. CONTROL SYSTEM ..... 10

**2. MEASUREMENT CONDITIONS ..... 13**

2.1. ANKA LIGTH SOURCE CONDITIONS ..... 13

2.2. SETUP CONDITIONS ..... 14

**3. CALIBRATION AND CONDITIONING ..... 17**

3.1. CONDITIONING..... 17

3.2. CALIBRATION..... 18

**4. MEASUREMENT PROGRAM..... 20**

4.1. TEST PROGRAM..... 20

4.2. TESTS SCHEDULE ..... 21

**5. MEASUREMENTS ..... 22**

5.1. DATA..... 22

5.2. ANALYSIS AND DISCUSSION ..... 24

**6. CONCLUSIONS ..... 25**

**7. REFERENCES..... 26**

**ANNEX: GLOSSARY ..... 27**

## 1. DESCRIPTION OF THE TEST SETUP

The goal of the test setup is to determine the photodesorption yield, synchrotron radiation heat loads and photo-electrons generation inside the beam screen prototype. To this end, the prototype will be installed in a front end of the ANKA synchrotron ring and exposed to significant levels of synchrotron radiation, comparable to those expected at a 100 TeV hadron collider.

The EuroCirCol project proposal foresaw installing the Coldex setup of CERN[1] at ANKA, but already at the beginning of the project it was realised that the Coldex setup was not available for the experiment.

In order to be able to achieve the objective to experimentally determine the performance of the novel beam screen (BS) design, we decided to develop a dedicated BEam Screen Testbench EXperiment (BESTEX) setup specifically for the needs of the EuroCirCol project.

After several design iterations the measurements at BESTEX were decided to be limited to room temperature. This decision permits obtaining the required efficiency validation of the prototype at reduced complexity and cost. The design of BESTEX is, however, prepared for tests using liquid nitrogen as a coolant, at 77 K if needed.

### 1.1. ANKA LIGHT SOURCE

ANKA is a test facility and synchrotron radiation source at the Karlsruhe Institute for Technology (KIT). Synchrotron light is produced with an electron beam energy of 2.5 GeV and beam currents up to 200 mA (Figure 1) [2]. ANKA can also be operated with lower electron energies down to 0.5 GeV.



*Figure 1: ANKA Light Source*

The decision to use ANKA for the test of the FCC-hh beam screen was taken due to the similarity of the synchrotron light emission with FCC-hh, in terms of beam power and light spectrum. In Figure 2 it is shown the comparison of the emitted light at ANKA and the foreseen emission at FCC-hh [3].

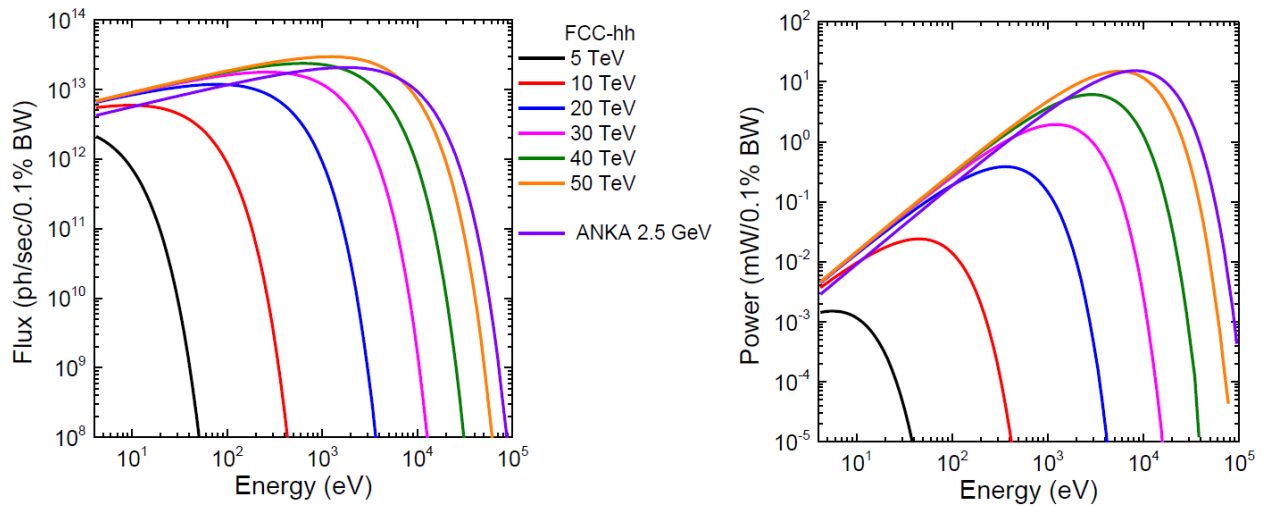


Figure 2 Synchrotron light emission at ANKA and FCC-hh as a function of photon energy and for different FCC-hh proton energy (left: Flux, right: Power).

Table 1: ANKA parameters and requirements for EuroCirCol; DP=dipole; SR=synchrotron radiation

ANKA Parameters		
Energy	2.5	GeV
Emittance	50	nm
Circumference	110.4	m
Current	200	mA
Optics	4x2	DBA
DP-Field	1.5	T
DP SR Power	18	W/mrad
DP SR Photon Flux	$6 \cdot 10^{19}$	Ph/(s mrad)
$E_{critic}$	6.2	KeV
FCC Parameters		
DP SR Power	32	W/m*
DP SR Photon Flux	$6 \cdot 10^{17}$	Ph/(s m*)
BESTEX Parameters (at ANKA after collimation)		
DP SR Power	32	W/m*
DP SR Photon Flux	$5 \cdot 10^{16}$	Ph/(s m*)
Incident angle	18	mrاد
<i>*m: irradiated length</i>		

## 1.2. BESTEX

### 1.2.1 FRONT END SETUP

In order to be able to irradiate the beam screen prototype with appropriate synchrotron light, a port with bending magnets was chosen. The port has to have enough beam aperture for a wide radiation fan to reach the prototype and there should be enough space for the installation of the foreseen two meter long screen prototype. Photons with similar energy spectrum and power as expected to impinge on the FCC-hh arc vacuum chamber are extracted from one of the ANKA bending magnets using a fixed aperture crotch absorber.

The chosen beam port is marked with a red dot in Figure 3.

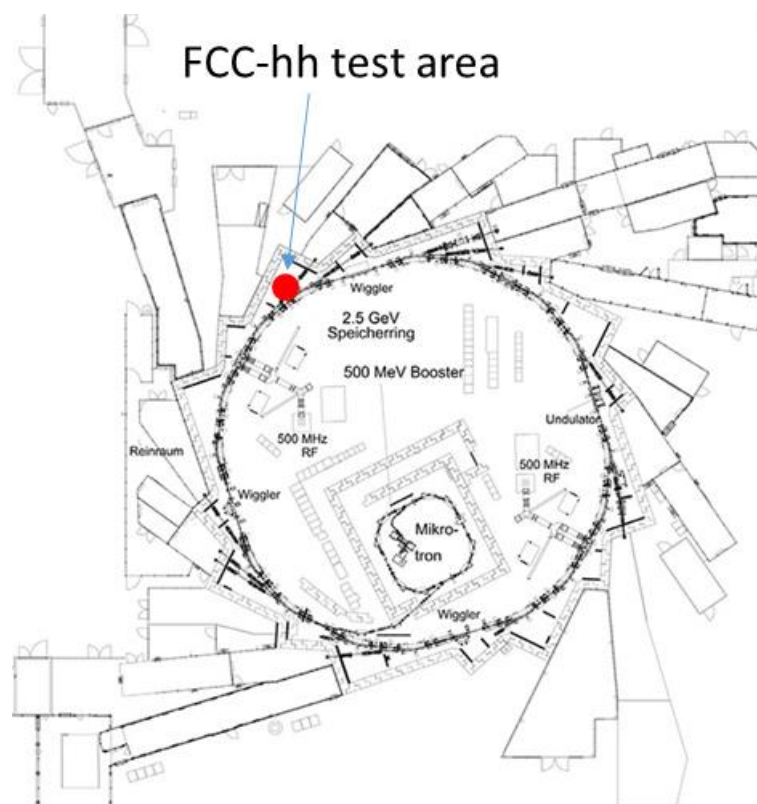


Figure 3 Location of the chosen front end, marked by red dot.

The front end has the function to allow the extraction of the synchrotron light and to isolate the experiment from the vacuum of the accelerator (see figure 4).

A sector gate valve allows to install and exchange the test stand without breaking the vacuum integrity of the ANKA storage ring.

A sector photon absorber allows to connect both ANKA's and BESTEX's vacuums while keeping the system free of radiation

The front end part is also equipped with a collimator, placed after the sector valve and absorber which counts two pairs of slits. These slits are movable both in the horizontal and vertical direction so that the shape and size of the incoming photon beam can be modified. By doing so we can control the geometry of the photon beam fan. Also, the photon flux and power can be controlled to some extent.



More in detail, the installed equipment includes (see Figure 4 and Figure 5):

- Crotch absorber, limiting the available photon aperture and absorbing the remaining synchrotron radiation power
- Ion vacuum pump, in order to pump down the desorption in the absorber.
- Vacuum gate valve, to isolate the storage ring vacuum from the experimental setup
- Photon absorber in order to keep the system free of radiation if needed
- Collimating Slits in order to control the incoming radiation

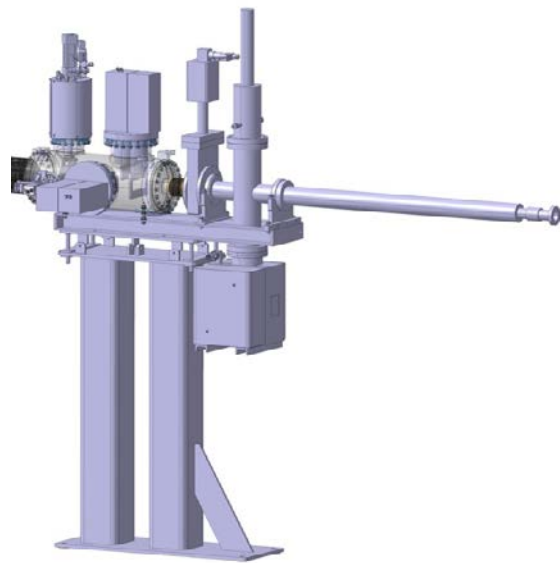


Figure 4: Front end components; **Left:** as installed at ANKA **Right:** 3D drawing of the components



## 1.2.2 MEASUREMENT SETUP

The measurement setup is shown in Figure 5 and Figure 6. It is composed of two main parts, the front end and the test bench, linked by a bellow. Figure 5 shows the 3D model of the installed test bench.

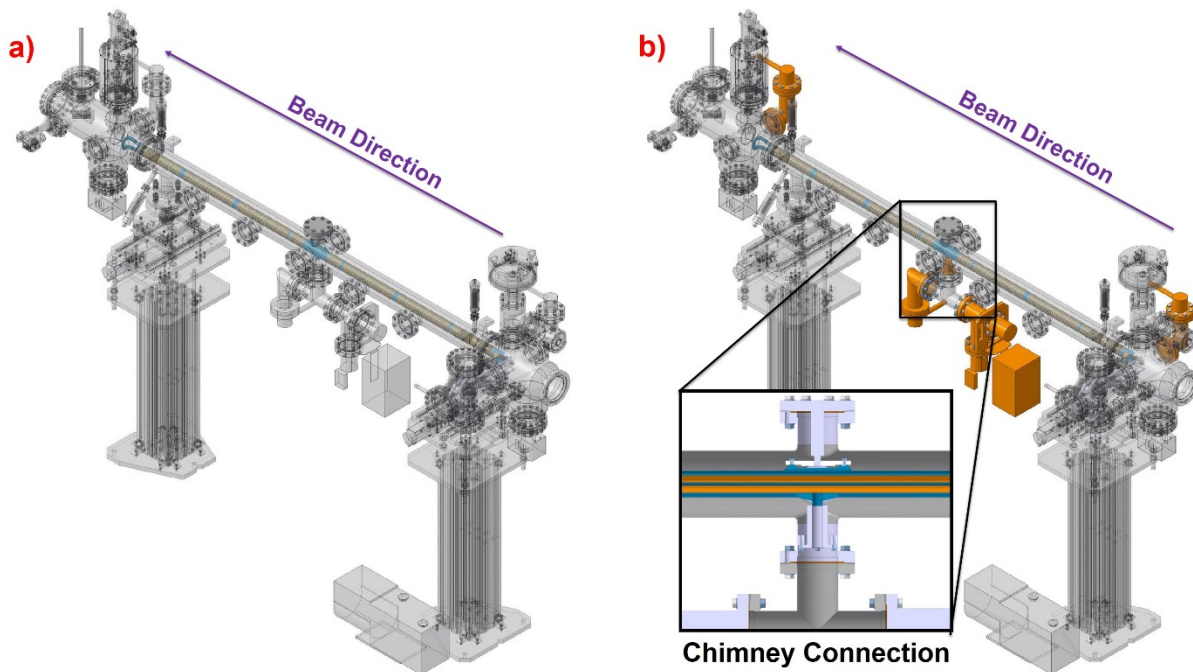


Figure 5 Drawing with the different component of the test setup

The setup is equipped with a residual gas analyser (RGA) and a series of Bayard Alpert pressure gauges (BAGs) strategically placed along the test bench, see orange highlighted parts in Figure 5b. Two BAGs are placed symmetrically at each extremity of the bench, named front and back BAG, respectively.

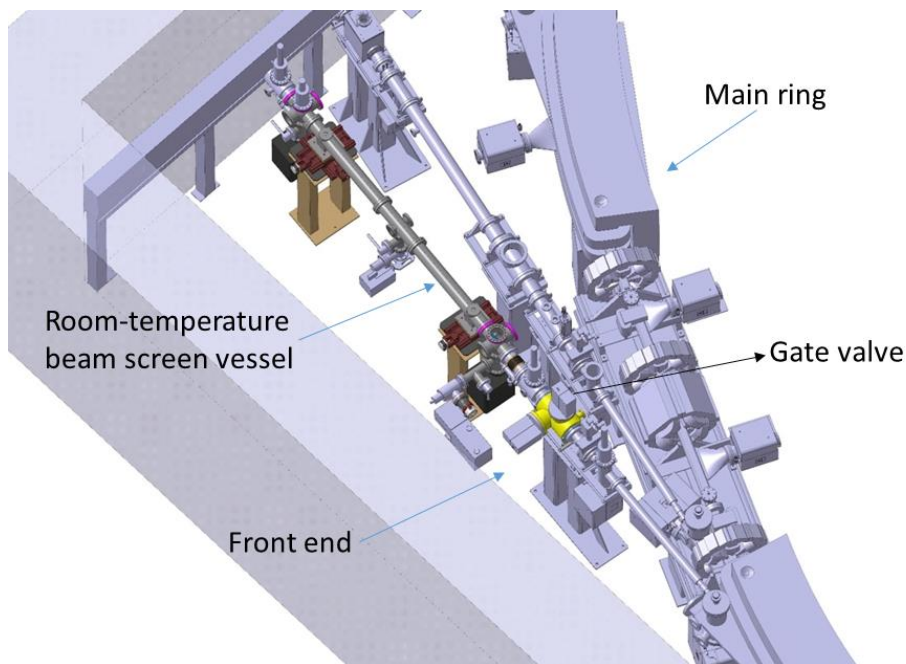


Figure 6 Implementation of the test setup in the ANKA facility

A third BAG (middle BAG) and an RGA are installed together in the middle instrumentation assembly, at the middle point of the setup. As shown in Figure 5b, the middle instrumentation assembly is connected to the interior part of the beam screen prototype through a chimney connection which allows direct pressure and gas analysis inside the test BS.

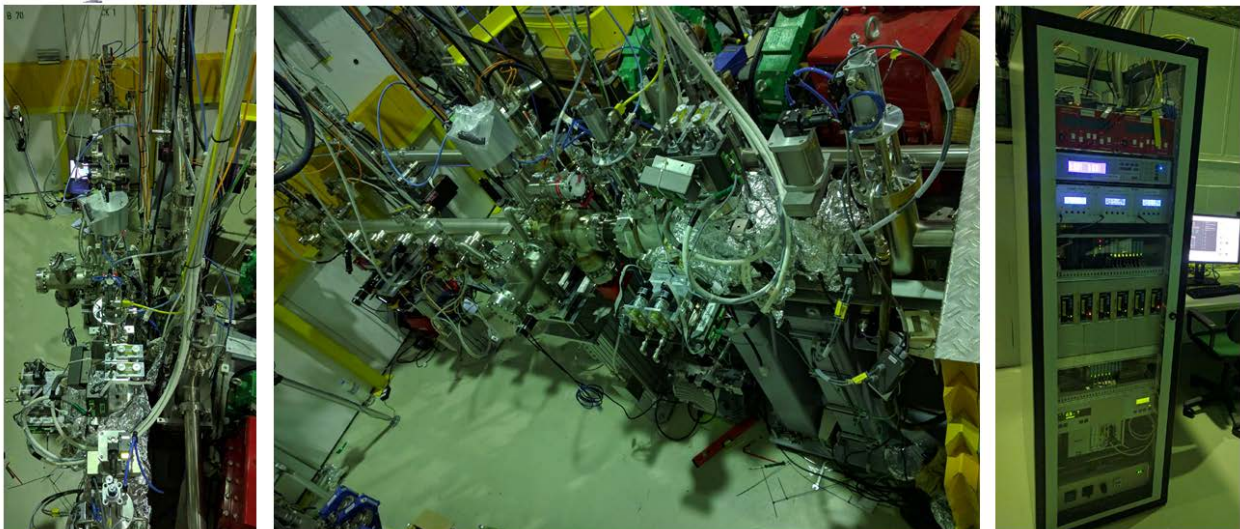


Figure 7 Pictures of the test setup in the ANKA facility

**Left:** Top view **Middle:** Side view **Right:** Control rack installed at ANKA

### 1.3. CONTROL SYSTEM

The control system of the test setup is based on the following equipment.

Two S7PLC (PLC: Programmable Logic Controller) are used to control all the instrumentation. The BESTEX's PLC code was written at CERN as well as the SCADA user interface. The ANKA PLC controls the sector valve and absorber. to satisfy the ANKA's safety interlocks logics. The BESTEX's PLC Input/output and PLCs communication scheme is shown in Figure 8.

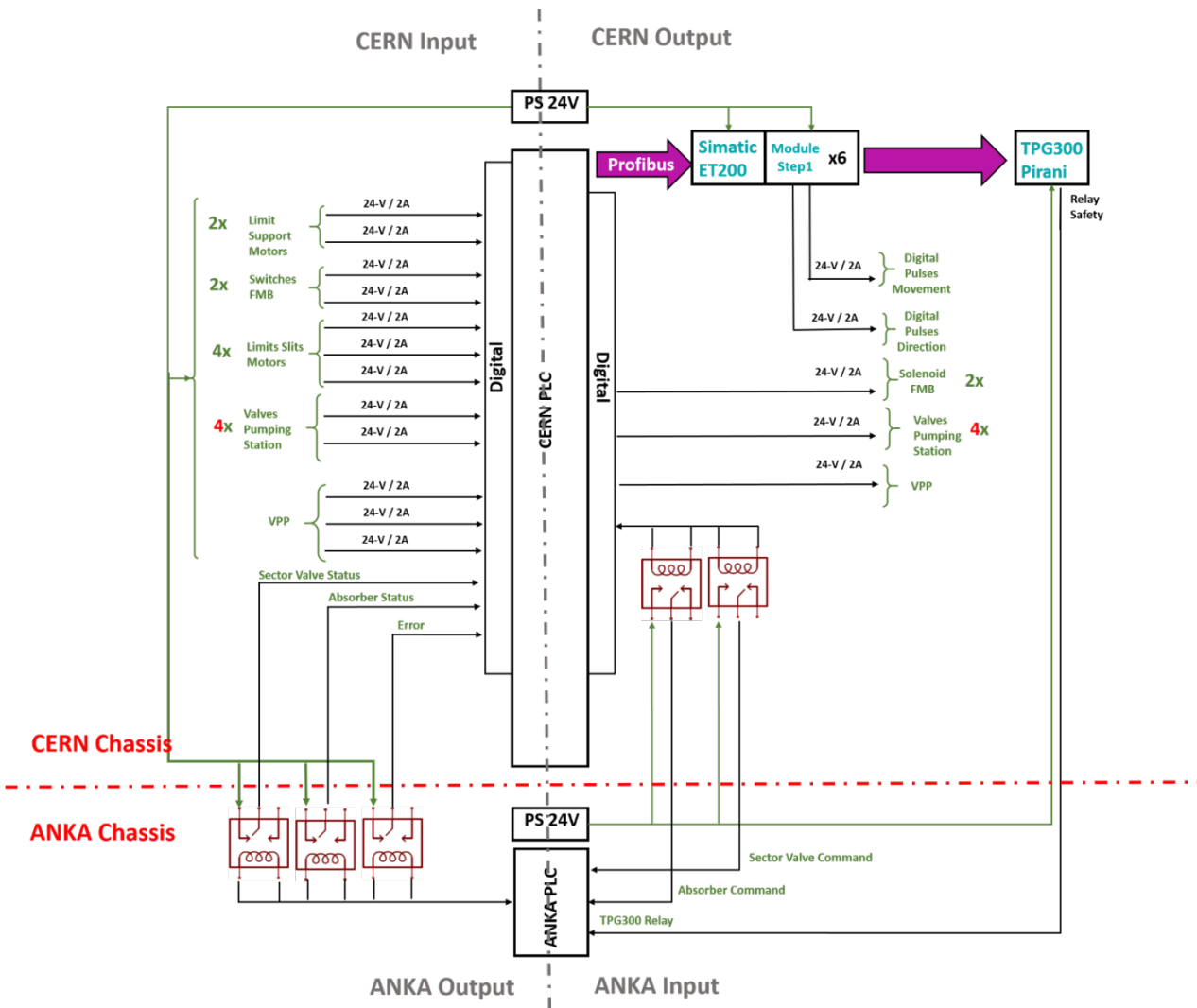


Figure 8: Scheme of the setup controls installation integrated in the BESTEX-ANKA system

A NI PXIe-8820 Dual-Core controller is used to perform the data acquisition with LabView. The labview code was developed at CERN based on the Producer/Consumer architecture called Queue Message Handler (QMH). A Virtual Instrument (VI) code was written for each of the devices generating data. Each VI runs independently while a main VI receives and manages the data provided by the different devices. The main VI then exports and saves the data synchronized with a timestamp chosen by the user. Communication between BESTEX's PLC and PXI is performed by using LibnoDave communication library. By doing so the status of the sector valve and absorber, as well as



motors and pumps can be synchronized with the LabView acquired data. A schematic description of the basic working principle of the BESTEX's LabView software is shown in Figure 9.

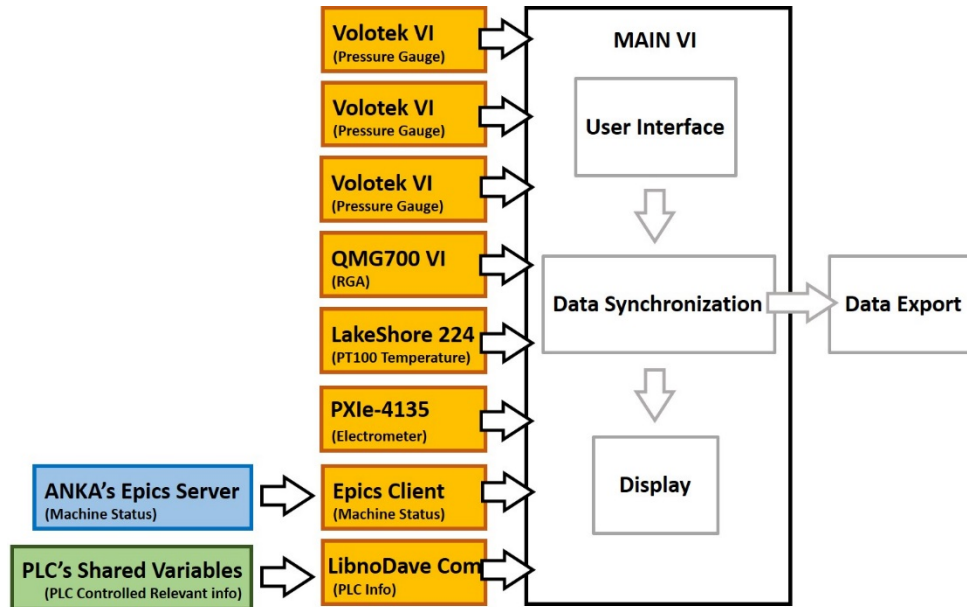


Figure 9 Scheme of the LabView Architecture integrated in the BESTEX-ANKA system

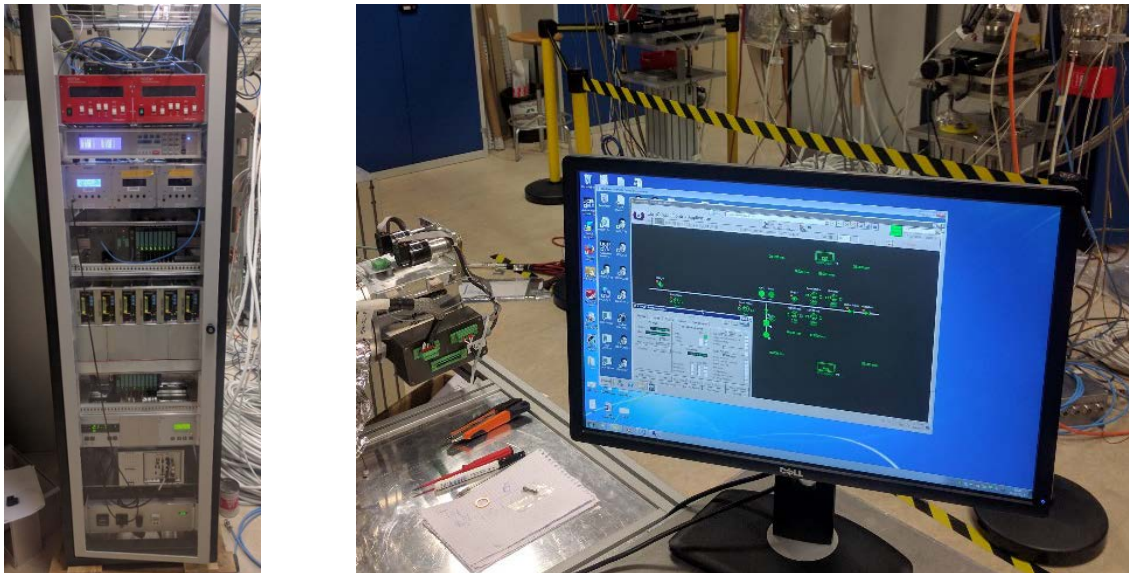


Figure 10 Left: BESTEX Control rack. Right: BESTEX SCADA application

The hardware required to operate the test setup is installed in the ANKA hall in controls rack (see picture 10), and it is composed of :

- Siemens S7-200 PLC
- 6 x Simatic ET200 Stepper Motor Module
- TPG300 Pirani+Penning gauge controller

- 3 x Volotek Bayard Alpert gauge controller
- Lakeshore temperature sensor controller
- 6 x Middex BCD130 step motor driver
- TCP 350 Turbo Pump controller
- 2 x NIOPS NexTorr controller
- Scroll roughing pump controller
- PXIe-8820 Dual-Core

## 2. MEASUREMENT CONDITIONS

### 2.1. ANKA LIGHT SOURCE CONDITIONS

The ANKA light source will operate under its nominal conditions for emittance (defining the beam size and divergence) and energy (2.5 GeV [5]). Table 2 shows the nominal operating parameters. ANKA works in a so called “current decay mode”. The electron beam is injected twice a day to a maximum average beam current up to 200 mA decreasing down to 100-50 mA before the next injection.

*Table 2* Nominal parameters of ANKA[5]

Parameter		Unit
Energy	0.5-2.5	GeV
Circumference	110.4	m
Number of dipoles	16	
Dipole field	1.5	T
Number of quadrupoles	40	
Maximum gradient	18	T/m
Number of sextupoles	24	
Maximum gradient	520	T/m <sup>2</sup>
Number of correctors, h/v	28/16	
Maximum kick strength, h/v	1/1	mrad
Momentum compaction factor	0.008	
Natural Chromaticity	-17/-8	
Energy spread	0.001	
Emittance	40-70	nm rad
Max. overvoltage factor	3.6	
Energy lost per turn	622	keV
Maximum RF voltage/cavity	560	kV
Photon critical energy	6	keV

The beam source parameters at the bending magnet are given in Table 3.

*Table 3* Beam parameters at the bending source point

Horizontal size	245	μm
Horizontal divergence	179	μrad
Vertical size	83	μm
Vertical divergence	4	μrad

The spatial spectral power and flux distributions of the photon beam after the crotch absorber are shown in Figure 11

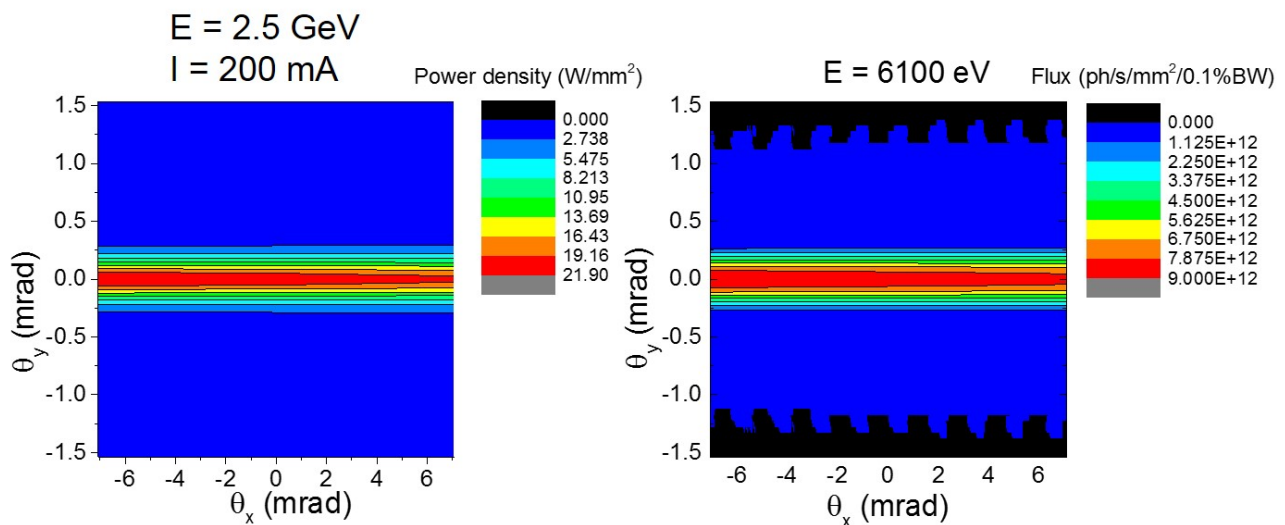


Figure 11 Spatial spectral distribution; Left: power at E=2.5GeV and I=200mA electron beam. Right: Flux at 6100 eV photon energy;

## 2.2. SETUP CONDITIONS

The sample under measurement is a 2 meter long prototype (Figure 11), the length is needed in order to be able to irradiate only the central part and avoid spurious effects due to the impact of primary, un-scattered radiation onto the end parts of the sample.



Figure 12 Finalized beam-screen prototype. Photo taken prior to shipment to ANKA

In order to precisely control the irradiated region

it is of great importance an accurate alignment of the sample screen with respect to the photon beam plane. The remote horizontal motion of the BS sample is needed to change the irradiated area with beam. The collimator was set at an aperture of 1.11 mm in the vertical direction and 20.39 mm in the horizontal direction. Such aperture leads to a total flux of  $8.73E16$  photons per second and a total power of 56.40W across the collimator.. In figure 13a, it is shown the condition in which the screen is completely parallel to the synchrotron radiation. In this condition the screen is not irradiated. By tilting the beam screen by an angle of 18 mrad, the irradiation pattern onto the screen in the central part covers 1.8 meters (some scattered photons may hit outside of this length), leaving 10 cm before and after to avoid direct end effects (see Figure 13 b). This geometry leads to a power density of 31.3W/m, which is in good agreement with the expected value for FCChh [6]



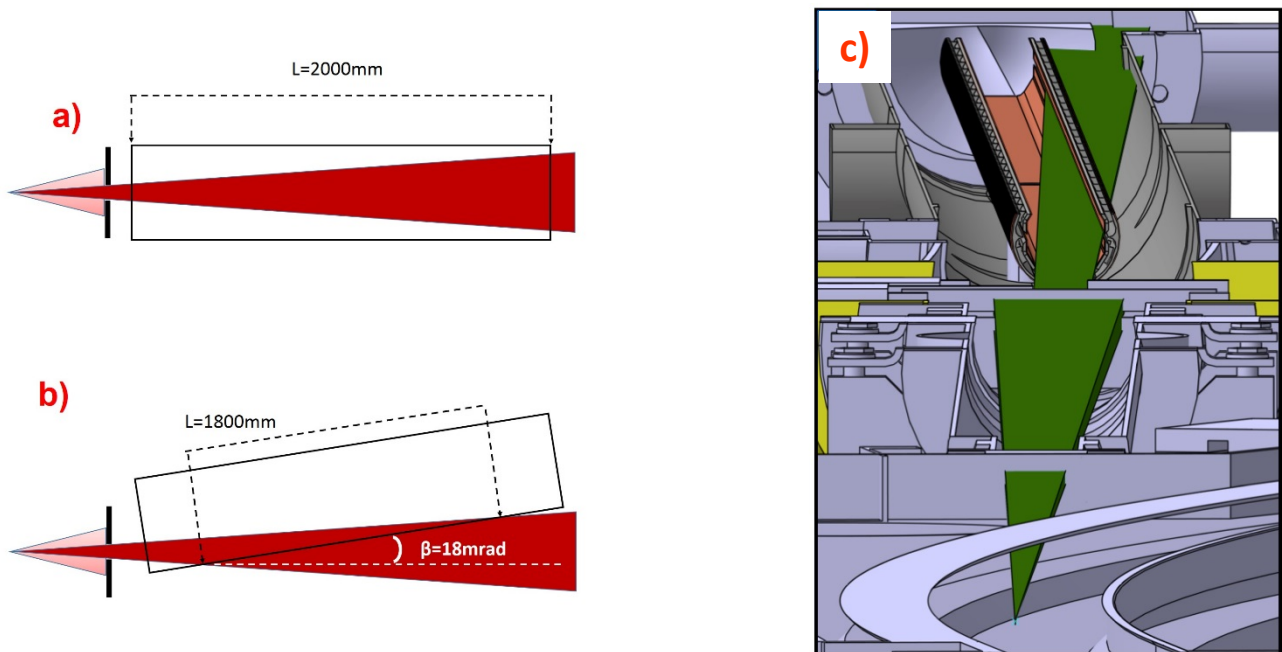


Figure 13 a) Beam screen parallel to the SR beam b) Tilted screen for irradiation tests. c) Ray tracing computation

This alignment conditions have been checked with ray tracing computations with the real dimensions and conditions of the ANKA storage ring, figure 13c. In order to ensure the above conditions in the experimental setup, an accurate knowledge of the beam screen position inside the vacuum chamber with respect to the fiducials placed on the outside, is required. For that, the position of the screen has been fiducialized by using micrometer positioning actuators, see Figure 14.

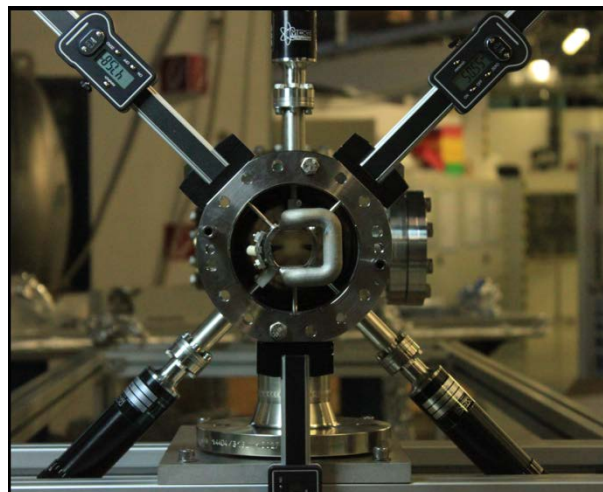


Figure 14 Beam screen aligned inside the vacuum chamber with micrometer actuators.

Repeated measurements provide a total accuracy of less than 0.7 mm, enough to ensure a precise irradiation into the deflector of the screen, Figure 15.

Manufacturing - Reflector Position < 0.500mm  
 Caliper method - Repeatability < 0.050mm  
 Laser Tracker alignment BS- Accuracy < 0.200mm  
 Laser Tracker alignment Slits- Accuracy < 0.200mm

**$\Delta < 0.700 \text{ mm}$**

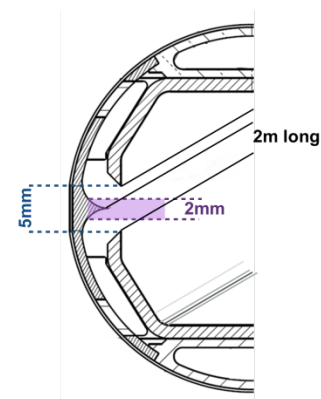


Figure 15 Accuracy measured <0.7 mm, inside the 2 mm margin for the photon deflector

Finally, to ensure the proper dimensions of the photon fan impinging onto the beam screen, the collimators of the front end have to be controlled remotely.

### 3. CALIBRATION AND CONDITIONING

The installation of the whole test bench was carried out during two long shutdowns of the ANKA light source, 1<sup>st</sup> and 2<sup>nd</sup> week of April and 3<sup>rd</sup> week of May.

During the first shut down the entire control system was installed and commissioned. This included the installation of the rack, the cables testing of all devices and the testing of the communication with the ANKA's control PLCs for correct interlock management. The test bench support was aligned using a laser tracker.

During the second shut down the test bench was installed and aligned, with respect to the ANKA's beam plane by using a laser tracker. After bake out, the system was confirmed to be leak tight at a leak rate of  $1\text{E-}10$  mbar·l/s.

#### 3.1. CONDITIONING

During the experiment, in order to reduce the outgassing originated at the light collimator, the latter was conditioned prior to irradiation of the beam-screen prototype. The SR flux and power follow a pseudo-gaussian distribution in the vertical direction as derived from Figure 11. In order to maximise the photon dose in the the largest aerea possible, the slits were moved during irradiation.

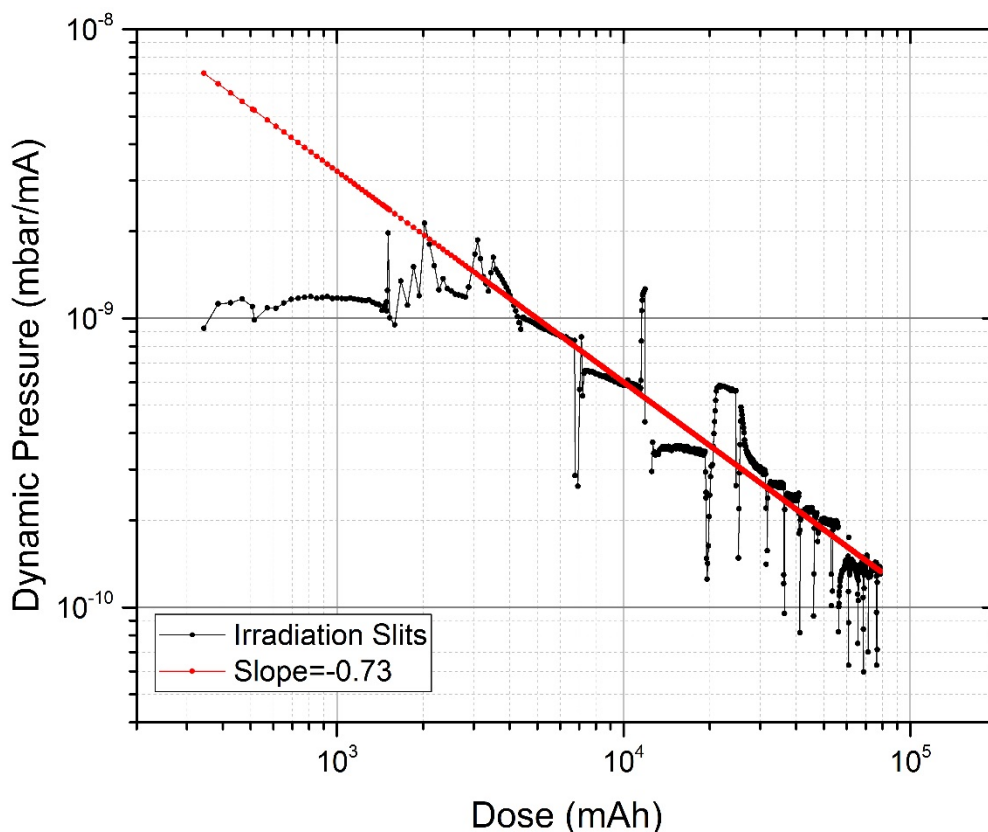


Figure 16 Conditioning curve resulting from the irradiation of the collimator; Black: data; Red: power-law fit  $P \propto D^\alpha$ .

The conditioning curve obtained is shown in Figure 16. The graph shows a very noisy behaviour. This effect is ascribed to the movement of the collimator. During conditioning, at each of its positions, the

collimator reflects the photons in different directions, and due to this the number of reflected photons impinging on the walls of the vacuum chamber might drastically differ between different geometries. Besides, as the collimator moves, the calculated photon dose is not as accurate as it would be for a stationary system. A main tendency following a power law  $P \propto D^\alpha$  with a slope  $\alpha = -0.73$  is observed. The conditioning process was carried out until a stable pressure was achieved. Final pressures in the system after the conditioning process are presented in Table 4.

Table 4 Beam parameters at the bending source point

Beam Current (mA)	Front (mbar)	Middle (mbar)	Back (mbar)
145	1.4E-9	1.7E-9	5.7E-10
60	1.0E-9	1.2E-9	4.5E-10

### 3.2. CALIBRATION

Movable fluorescent screens are used to crosscheck the correct aperture and position of the beam collimator. Figure 17 shows a comparison of the footprint originated, for the same collimator aperture, at the fluorescent screen located at the back end of the bench, both in the ideal case (according to the system 3D model) and the real case (as observed while irradiation with ANKA light).

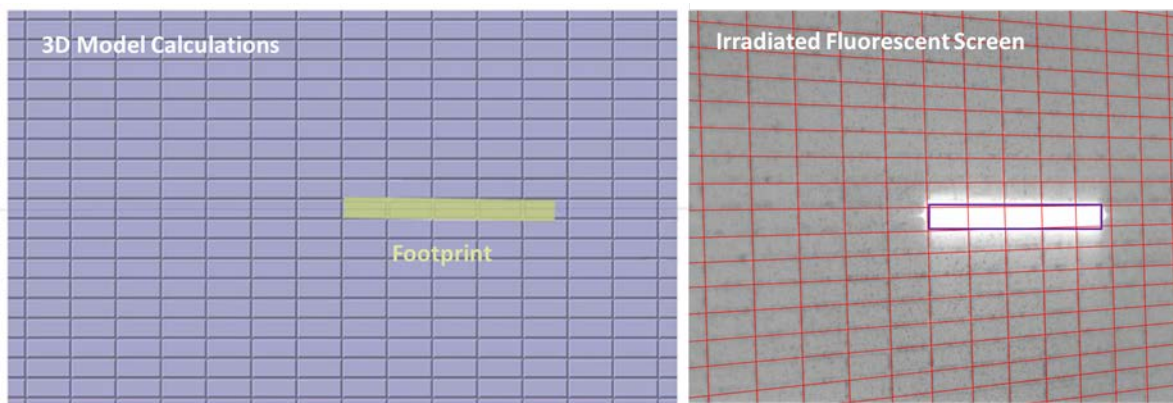


Figure 17 Synchrotron radiation footprint of back fluorescent screen after collimation. Comparison between **Left**: 3D model calculation. **Right**: Experimentally observed footprint

The observed correlation between the theoretical and observed footprints proves a well modeled and aligned setup. The setup was aligned according to the theoretical position of the beam plane. The beam plane corresponds to the geometrical location of the maximum value of the power distribution (see Figure 11). In order to validate the correct alignment of the complete system, taking also into account the SR beam spatial power distribution, the collimator was set at a gap of 0.5 mm and the position of its center was changed performing scans in the vertical direction as described in Figure 18 b.

The collimated beam was impinging on the back fluorescent screen without directly hitting the BS prototype. During the performance of a complete vertical stroke, the collimator gap scans the whole SR power distribution and the pressure in the system behaves accordingly.

The scans were performed in both the positive and negative directions from -5mm to +5mm and backwards, being 0 mm the position coincident with the theoretical position of the beam plane, to which the whole setup was aligned..

The evolution of the pressure is presented in Figure 19. as a function of the position of the center of the collimator gap

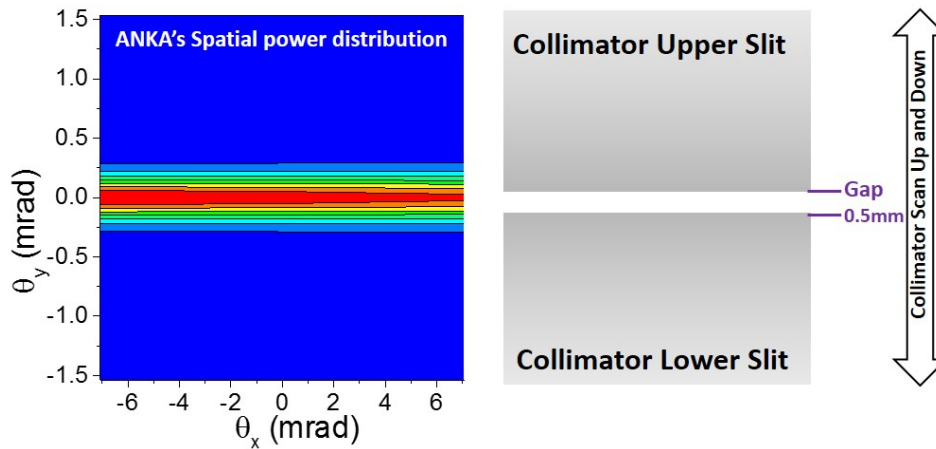


Figure 18 Schematic description of the geometry of the collimator and the spatial power distribution during collimator scans

It can be observed that as the gap approaches the beam plane (collimator gap center at 0 mm) the pressure in the system rises. In both cases, positive and negative direction scans, two narrowly-separated peaks can be observed, which are at coincident positions for both scans and are separated by  $\sim 0.5$  mm, in good agreement with the collimators gap aperture. These two peaks are understood to be originated by photons emitted on the electron beam orbit plane (highest flux and power) which are reflected by the edges of the collimator. The latter are machined but have a tiny residual curvature. The beam plane is therefore assumed to be located at the middle point between these two peaks. This analysis shows that the beam plane is coincident with the theoretical position within the limits of our alignment tolerances discussed above.

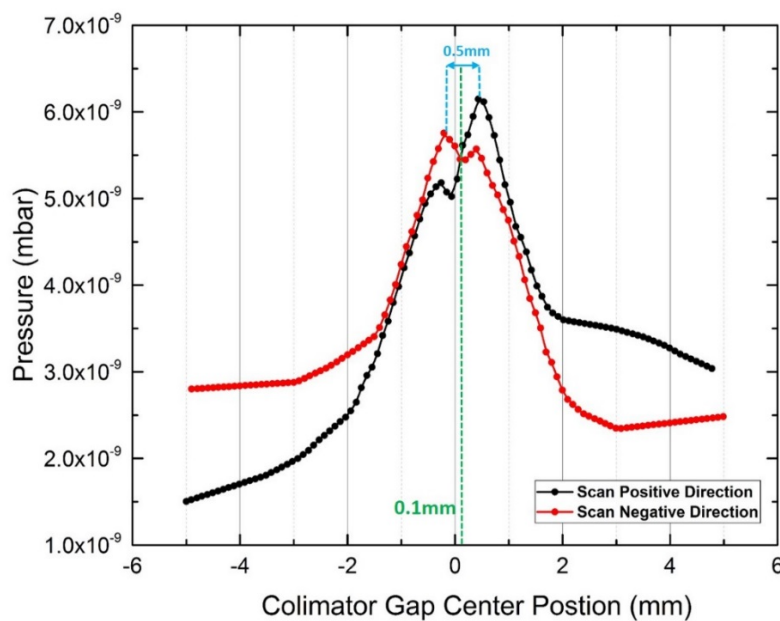


Figure 19 Evolution of pressure during Collimator scans

## 4. MEASUREMENT PROGRAM

### 4.1. TEST PROGRAM

The setup at ANKA will measure the following parameters of the beam screen prototype:

- Photo desorption yields as a function of photon dose  
The molecules desorbed inside the beam screen prototype by synchrotron radiation are detected through the chimney connected via the central port of the beam screen prototype by using a BAG and an RGA quadrupole mass spectrometer in order to measure the induced pressure rise and to characterise the composition of the desorbed gas species.
- Heat load distribution  
A series of PT100 resistive temperature sensors are installed along the beam screen prototype at some relevant positions, so as to qualify the thermal properties of the prototype and compare the temperature distribution to finite-element and ray-tracing thermal calculations.
- Reflectivity and efficiency of the photon deflector  
A positively biased wire electrode is installed in front of the photon collector, immediately after the BS. The photoelectron current due to the irradiation with synchrotron radiation will be measured in two cases: a) direct incidence of the light onto the collector; b) “nominal” incidence of the light into the deflector of the BS prototype. The different amount of photoelectrons generated at the collector is expected to provide information about the light deflecting efficiency of the beam screen prototype.
- Photoelectron yield  
Thin copper electrodes will be placed in the inner part and all along one of the BS prototypes. They will be electrically isolated from the BS prototype itself via thin sprayed ceramic films. By biasing the electrodes positively, photoelectrons will be measured as the synchrotron radiation impinges onto the deflector.



## 4.2. TESTS SCHEDULE

The test program spans from March 2017 until June 2018 with the foreseen schedule as shown in Figure 20.

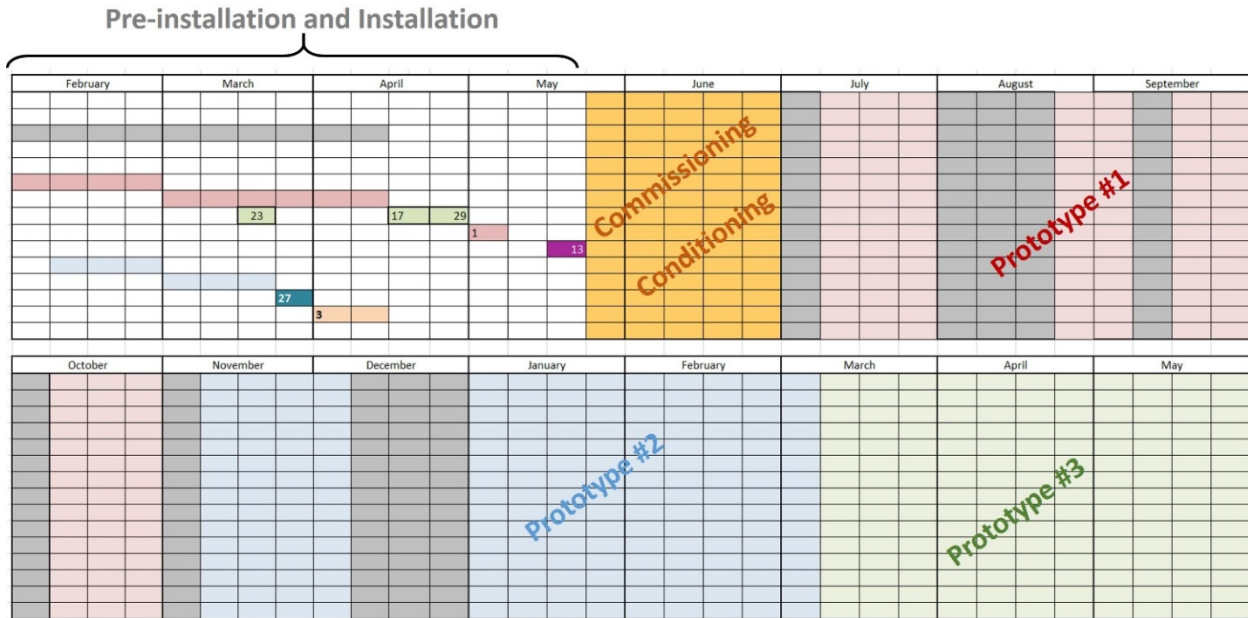


Figure 20 Planing of measurements



## 5. MEASUREMENTS

### 5.1. DATA

Irradiation of the first prototype has started on 19<sup>th</sup> of July with the ANKA light source working at 2.5 GeV and an average current of 130 mA. Up to date a total dose of  $2.5E22$  ph/m was accumulated on the first beam screen prototype. Figure 21 shows the evolution of the pressures in the system during the whole irradiation period. The values of the pressures have been normalized to the electron beam current and are expressed in [mbar/mA]. It should be noted that the static pressure of each gauge, before irradiation, is subtracted from these pressure values, so as to put in more evidence the contribution due to synchrotron radiation-induced desorption (sometimes referred to in the literature as photon-induced desorption (PID) or photon-induced yield (PIY)).

During the first cycles, pressures at the front and back gauges of the sample remained similar and lower than the pressure measured through the chimney, which indicates that the radiation impinged entirely on the sample, and denotes a proper alignment.

The results show that for photon doses higher than  $\sim 1E20$  ph/m the pressure decreased with a slope of  $\alpha \sim -0.5$  for the back and middle BAGs as expected from literature results [7,8], indicating a parallel pressure decreasing trend. Due to the limited pumping speed inherent to the setup geometry, and the limited conductance of the BS geometry, the pressure measured through the chimney is always higher than for the front and back BAGs.

It can be observed that the reading of the front gauge shows a slower pressure decreasing rate. While both front and back gauges show similar readings at low photon doses, as the photon dose increases, the pressure at the front gauge tends to remain higher than that at the back gauge, resulting in a slope of  $\alpha \sim -0.37$ .

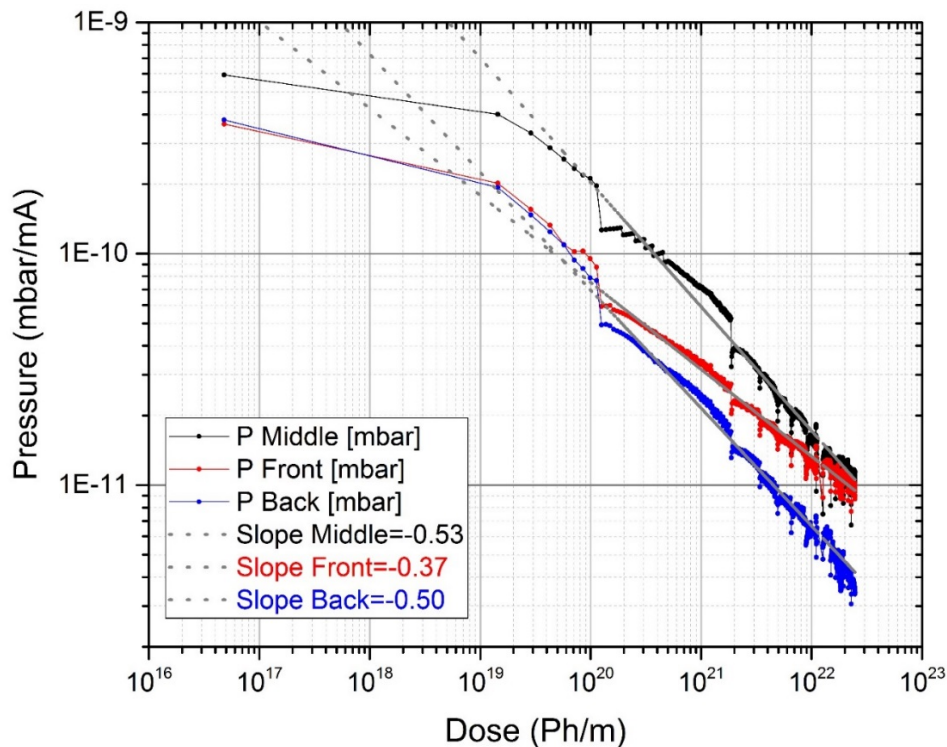


Figure 21 Pressure evolution measured at BESTEX setup during irradiation through the chimney (black), at Front gauge (Red) and Back gauge (Blue). Gray dotted lines represent the fitting power function,  $P \propto D^\alpha$ .

Table 5 shows relevant comparison between the pressure measured at the back BAG during the last cycle of the experiment (at 2.5 GeV) with the pressure measured at the front BAG after the collimator conditioning process. In both cases the electron beam current was 145 mA

Table 5 Beam parameters at the bending source point

BAG	Beam Current (mA)	Front (mbar)
Front	145	1.4E-9
Back	145	7.9E-10

The behavior observed for the pressure measured at the front gauge was attributed to the outgassing originated at the photon beam collimator, which due to its proximity to the front BAG, contributes to the pressure reading.

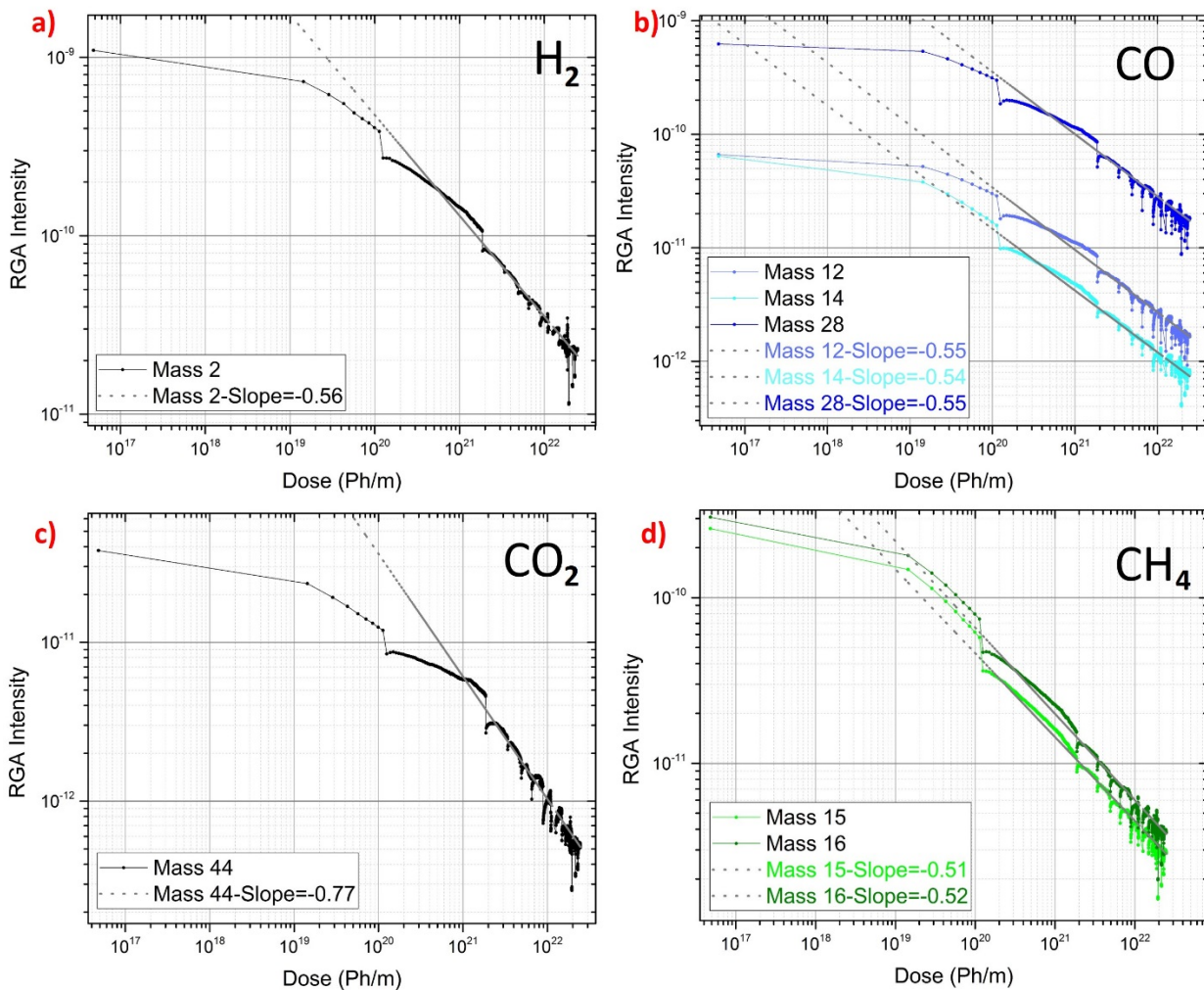


Figure 22 Evolution of RGA measured signals at BESTEX setup during irradiation through the chimney. a) Results for masses corresponding to H<sub>2</sub>. b) Results for masses corresponding to CO. c) Results for masses corresponding to CO<sub>2</sub>. d) Results for masses corresponding to CH<sub>4</sub>. Gray dotted lines represent the corresponding fitting power functions.

The slits which collimate the incoming photon beam, when closed at 2 mm vertical opening, crop 83% of the total flux and 69% of the total power. After conditioning of the collimator, when no further significant decrease in pressure was observed, the front BAG showed a pressure of 1.4E-9 mbar, which is somewhat higher than the expected contribution from the beam screen prototype at high doses i.e.  $\sim 7.9E-10$  mbar, as measured at the back BAG. Due to this fact and despite the previous conditioning, the contribution of molecules originated at the collimator begins to become predominant as the BS prototype is conditioned, resulting in a smaller pressure decreasing rate.

Figure 22 shows the evolution of the measured RGA intensities, normalised to the electron beam current. The characteristic masses of H<sub>2</sub>, CO, CO<sub>2</sub> and CH<sub>4</sub> are represented separately. For photon doses higher than 1.0E21ph/m the curves' trend decrease continuously with an absolute value of the slope always higher than 0.5 in good agreement with relevant literature results [6,7].

## 5.2. ANALYSIS AND DISCUSSION

A preliminary comparison of the measured pressure results with respect to the predicted ones is shown in Table 6 Experiment vs. computed results.. Experimental values of the pressure at middle, front, and back BAGs have been compared with their simulated counterparts for doses of 3.0 A•h and 9.5 A•h at 2.5 GeV electron beam energy. In order to be able to compare the data, they have been scaled to 130 mA.

*Table 6 Experiment vs. computed results*

	2.5GeV/130mA					
	3Ah			9.5Ah		
	Experiment	Simulations	Rel Discrepancy %	Experiment	Simulations	Rel Discrepancy %
Middle	7.25E-09	2.30E-08	68.5%	3.71E-09	1.20E-08	69.0%
Front	3.87E-09	4.70E-09	17.7%	2.44E-09	2.80E-09	12.9%
Back	2.42E-09	3.80E-09	36.4%	1.39E-09	2.00E-09	30.3%

The relative discrepancy between measured and simulated values of the pressure (1-Experiment/Simulations) for front and back pressures are around 15~35% which is comparable with the systematic error of the measurement of a BAG. In the case of the middle BAG however, the relative discrepancy rises up to almost 70%. To find possible causes at the origin of this mismatch it is worth noting that:

- i) in the simulations carried out so far, the area around the chimney in the middle of the BS was considered leak tight. In the real system, and due to manufacturing/alignment issues, an annular opening larger than foreseen is present, which somewhat enhances the local escape probability of molecules at that point (i.e. some molecules may go undetected by the middle gauge);
- ii) in this experiment, the vertical collimation of the photon flux yielded *an equivalent* critical energy after the slits of 8020 eV (6230 eV before the slits), due the reduced flux of low-energy photons which are on average generated at larger vertical angles at the source point. The available PSD data used for the simulations is for 4.0 keV. The discrepancy observed between measurements and simulations might be attributed to the fact that for higher critical energies the yields can be smaller than for lower critical energies at high photon doses.

It is worthwhile noting that the simulations foresee a higher pressure reading at the front BAG due to the outgassing generated at the collimator, which as discussed above is confirmed by the experimental results.

## 6. CONCLUSIONS

The test campaign at ANKA has started and will continue until June 2018 or beyond, if deemed necessary and possible.

After irradiation of the fluorescent screens, the validity of the alignment was confirmed and a correct 3D CAD modelling of the setup was validated. A preliminary analysis of the acquired data has been presented. The analysis reveals that, as expected from simulations the pressure measured at the middle BAG remains always higher than that of the front and back gauges. The relative discrepancies between experiment and simulations for front and back pressures are around 30% which is comparable with the systematic error of the measurement of a BAG. However, the relative discrepancy between experimental and simulated values for the pressures at the middle BAG are larger than those for back and front BAGs. Future simulations, will implement the real geometry in the model..

According to simulations, the pressure at front BAG has been measured to be higher than for the back BAG due to the outgassing originated at the collimator. As a consequence of the contribution of the molecules desorbed from the collimator, for photon doses higher than  $1E20$  ph/m, the normalised pressure at the front BAG decreases with a power law with a slope of  $-0.33$  which is considerably smaller than that of the back and middle BAGs ( $\sim -0.50$ ).

The evolution of the measured RGA intensities show a behaviour in good agreement with that expected from literature results [7,8].

For the remainder of this experimental run, before the BS is replaced with the next one, we are planning to change the photon irradiation pattern on the BS walls. In particular, we want to open up vertically the photon fan so to irradiate with primary photons one of the vertical parts of the BS. This is very important, because it would represent the condition of FCC-hh during the energy ramp-up (when the lower beam energy generates synchrotron radiation photons at larger vertical angles) or vertical misalignments of the BS (or entire dipole magnets) in the tunnel.

Further and more detailed data analysis and simulations as well are going to be carried out at the end of the first beamscreen prototype measuring campaign including the accurate estimation of residual gas composition.

## 7. REFERENCES

- [1] V. Baglin et al., "First results from COLDEX applicable to the LHC cryogenic vacuum system", THP1B03, EPAC '00.
- [2] H.O. Moser et al, "ANKA, a Synchrotron Light Source for Microstructure Fabrication and Analysis", Proceedings PAC95.
- [3] S. Casalbuoni et al, "FCC-hh Synchrotron Radiation Effects: The new ANKA facility for desorption measurement", presented at the FCC Week Conference 2016, Rome, Italy, 2016.
- [4] F. Perez and P. Chiggiato, 'Design, Prototyping and Tests of the FCC-hh Vacuum Beam Screen', presented at the FCC Week Conference 2016, Rome, Italy, 2016.
- [5] D. Einfeld et al. "Commissioning of the ANKA Storage Ring", Proceedings of EPAC 2000, Vienna, Austria, 2000.
- [6] Ignasi Bellafont "Photon ray tracing and gas density profile in the FCC-hh", FCC Week Conference 2017, June 1<sup>st</sup> 2017. Berlin, Germany.
- [7] O. Gröbner et al., "Gas desorption from an oxygen free high conductivity copper vacuum chamber by synchrotron radiation photons" Journal of Vacuum Science and Technology A
- [8] C.H. Falland et al., Proc 8th Int. Vacuum Congress, Cannes

## ANNEX: GLOSSARY

<b>Acronym</b>	<b>Definition</b>
<b>BAG</b>	Bayard Alpert Gauge
<b>BS</b>	Beam Screen
<b>c.m.</b>	Centre of Mass
<b>FCC</b>	Future Circular Collider
<b>FCC-hh</b>	Hadron Collider within the Future Circular Collider study
<b>FODO</b>	Focusing and defocusing quadrupole lenses in alternating order
<b>HE-LHC</b>	High Energy - Large Hadron Collider
<b>HL-LHC</b>	High Luminosity – Large Hadron Collider
<b>IBS</b>	Intra Beam Scattering
<b>IP</b>	Interaction Point
<b>KIT</b>	Karlsruher Institut für technologie
<b>LHC</b>	Large Hadron Collider
<b>Nb3Sn</b>	Niobium-tin, a metallic chemical
<b>Nb-Ti</b>	Niobium-titanium, a superconducting alloy
<b>RF</b>	Radio Frequency
<b>RGA</b>	Residual Gas Analyzer
<b>RMS</b>	Root Mean Square
<b>SR</b>	Synchrotron Radiation
<b>SSC</b>	Superconducting Super Collider
<b>UHV</b>	Ultra High Vacuum
<b>VI</b>	Virtual instrument